

The missing link: discerning true from false negatives when sampling species interaction networks

Michael D. Catchen^{1,2} Timothée Poisot^{3,2} Laura J. Pollock^{1,2} Andrew Gonzalez^{1,2}

¹ McGill University ² Québec Centre for Biodiversity Science ³ Université de Montréal

Correspondance to:

Michael D. Catchen — michael.catchen@mcgill.ca

Abstract: Ecosystems are composed of networks of interacting species. These interactions allow communities of species to persist through time through both neutral and adaptive processes. Despite their importance, a robust understanding of (and ability to predict and forecast) interactions among species remains elusive. This knowledge-gap is largely driven by a shortfall of data—although species occurrence data has rapidly increased in the last decade, species interaction data has not kept pace, largely due to the effort required to sample interactions. This means there are many interactions between species that occur in nature, but we do not know these interactions occur because we have never observed them. These so-called “false-negatives” bias data and hinder inference about the structure and dynamics of interaction networks. Here, we demonstrate the realized rate of false-negatives in data can be quite high, even in thoroughly sampled systems, due to the intrinsic variation in abundances across species in a community. We illustrate how a null model of occurrence detection can be used to estimate the false-negative rate in a given dataset. We also show how to directly incorporate uncertainty due to observation error into model-based predictions of interaction probabilities between species. One hypothesis is that interactions between “rare” species are themselves rare because these species are less likely to encounter one-another than species of higher relative abundance, and that this can (in part) explain the common pattern of nestedness in bipartite interaction networks. However, we demonstrate that across several datasets of spatial or temporally replicated networks, there are positive associations between species co-occurrence and interactions, which suggests these interactions among “rare” species actually exist but simply are not observed. Finally, we assess how false negatives influence various models of network prediction, and recommend directly accounting for observation error in predictive models. We conclude by discussing how the understanding of false-negatives can inform how we design monitoring schemes for species interactions.

1 Introduction

2 Species interactions drive many processes in evolution and ecology. A better understanding of species
3 interactions is an imperative to understand the evolution of life on Earth, to mitigate the impacts of
4 anthropogenic change on biodiversity (Makiola *et al.* 2020), and for predicting zoonotic spillover of
5 disease to prevent future pandemics (Becker *et al.* 2021). At the moment we lack sufficient data to meet
6 these challenges (Poisot *et al.* 2021), largely because species interactions are hard to sample (Jordano
7 2016). Over the past few decades biodiversity data has become increasingly available through remotely
8 collected data and adoption of open data practices (Kenall *et al.* 2014; Stephenson 2020). Still, interaction
9 data remains relatively scarce because sampling typically requires human observation. This induces a
10 constraint on the amount, spatial scale, and temporal frequency of resulting data that it is feasible to
11 collect by humans. Many crowdsourced methods for biodiversity data aggregation (e.g. GBIF, eBird) still
12 rely on automated identification of species, which does not easily generalize to interaction sampling.
13 There is interest in using remote methods for interaction sampling, which primarily detect co-occurrence
14 and derive properties like species avoidance from this data (Niedballa *et al.* 2019). However, co-occurrence
15 itself is not necessarily indicative of an interaction (Blanchet *et al.* 2020). This is an example of semantic
16 confusion around the word “interaction”—for example one might consider competition a type of species
17 interaction, even though it is marked by a lack of co-occurrence between species, unlike other types of
18 interactions, like predation or parasitism, which require both species to be together at the same place and
19 time. Here we consider interaction in the latter sense, where two species have fitness consequences on
20 one-another if (and only if) they are in the sample place at the same time. In addition, here we only
21 consider direct (not higher-order) interactions.

22 We cannot feasibly observe all (or even most) of the interactions that occur in an ecosystem. This means
23 we can be confident two species actually interact if we have a record of it (assuming they are correctly
24 identified), but not at all confident that a pair of species *do not* interact if we have *no record* of those
25 species observed together. In other words, it is difficult to distinguish *true-negatives* (two species never
26 interact) from *false-negatives* (two species interact sometimes, but we do not have a record of this
27 interaction). For a concrete example of a false-negative in a food web, see fig. 1. Because even the most
28 highly sampled systems will still contain false-negatives, there is increasing interest in combining
29 species-level data (e.g. traits, abundance, range, phylogenetic relatedness, etc.) to build models to predict

30 interactions between species we haven't observed together before (Strydom *et al.* 2021). However, the
31 noise of false-negatives could impact the efficacy of our predictive models and have practical
32 consequences for answering questions about interactions (de Aguiar *et al.* 2019). This data constraint is
33 amplified as the interaction data we have is geographically biased toward the usual suspects (Poisot *et al.*
34 2021). We therefore need a statistical approach to assessing these biases in the observation process and
35 their consequences for our understanding of interaction networks.

36 The importance of *sampling effort* and its impact on resulting ecological data has produced a rich body of
37 literature. The recorded number of species in a dataset or sample depends on the total number of
38 observations (Walther *et al.* 1995; Willott 2001), as do estimates of population abundance (Griffiths 1998).
39 This relationship between sampling effort and spatial coverage and species detectability has motivated
40 more quantitatively robust approaches to account for error in sampling data in many contexts: to
41 determine if a given species is extinct (Boakes *et al.* 2015), to determine sampling design (Moore &
42 McCarthy 2016), and to measure species richness across large scales (Carlson *et al.* 2020). In the context of
43 interactions, an initial concern was the compounding effects of limited sampling effort combined with the
44 amalgamation of data (across both study sites, time of year, and taxonomic scales) could lead any
45 empirical set of observations to inadequately reflect the reality of how species interact (Paine 1988) or the
46 structure of the network as a whole (Martinez *et al.* 1999; McLeod *et al.* 2021). Martinez *et al.* (1999)
47 showed that in a plant-endophyte trophic network, network connectance is robust to sampling effort, but
48 this was done in the context of a system for which observation of 62,000 total interactions derived from
49 164,000 plant-stems was feasible. In some systems (e.g. megafauna food-webs) this many observations is
50 either impractical or infeasible due to the absolute abundance of the species in question.

51 The intrinsic properties of ecological communities create several challenges for sampling: first, species are
52 not observed with equal probability—we are much more likely to observe a species of high abundance
53 than one of very low abundance (Poisot *et al.* 2015). Canard *et al.* (2012) presents a null model of food-web
54 structure where species encounter one-another in proportion to each species' relative-abundance. This
55 assumes that there are no associations in species co-occurrence due to an interaction (perhaps because
56 this interaction is “important” for both species; Cazelles *et al.* (2016)), but in this paper we later show
57 increasing strength of associations leads to increasing probability of false-negatives in interaction data,
58 and that these positive associations are common in existing network data. Second, observed co-occurrence
59 is often equated with meaningful interaction strength, but this is not necessarily the case (Blanchet *et al.*

2020)—a true “non-interaction” would require that neither of two species, regardless of whether they co-occur, ever exhibit any meaningful effect on the fitness of the other. So, although co-occurrence is not directly indicative of an interaction, it is a precondition for an interaction.

Here, we illustrate how our confidence that a pair of species never interacts highly depends on sampling effort. We demonstrate how the realized false-negative-rate of interactions is related to the relative abundance of the species pool, and introduce a method to produce a null estimate of the false-negative-rate given total sampling effort (the total count of all interactions seen among all species-pairs) and a method for including uncertainty into model predictions of interaction probabilities to account for observation error. We then confront these models with data, by showing that positive associations in co-occurrence data can increase the realized number of false-negatives and by showing these positive associations are rampant in network datasets. We conclude by recommending that the simulation of sampling effort and species occurrence can and should be used to help design surveys of species interaction diversity (Moore & McCarthy 2016), and by advocating use of null models like those presented here as a tool for both guiding design of surveys of species interactions and for including detection error into predictive models.

Accounting for false-negatives in species interactions

In this section, we demonstrate how difference in relative-abundance can lead to many false-negatives in interaction data. We also introduce a method for producing a null estimate of the false-negative-rate in datasets via simulation, and a method for incorporating uncertainty directly into predictions of species interactions to account for observation error.

How many observations of a non-interaction do we need to be confident it's a true negative?

We start with a naive model of interaction detection: we assume that every interacting pair of species is incorrectly observed as not-interacting with an independent and fixed probability, which we denote p_{fn} and subsequently refer to as the False-Negative-Rate (FNR). If we observe the same species not-interacting N times, then the probability of a true-negative (denoted p_{tn}) is given by $p_{tn} = 1 - (p_{fn})^N$. This relation (the probability-mass-function of geometric distribution, a special case of the negative-binomial

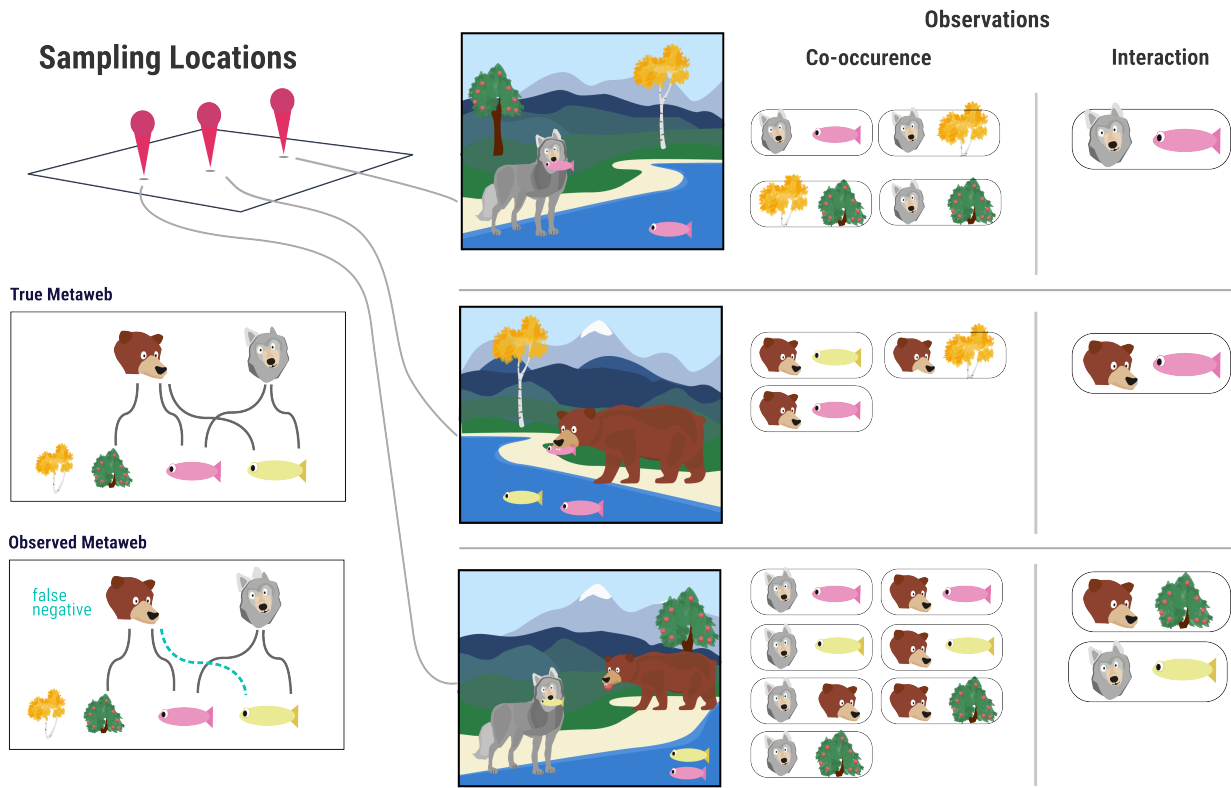


Figure 1: This conceptual example considers a sample of the trophic community of bears, wolves, salmon (pink fish), pike (yellow fish), berry trees, and aspen trees. The true metaweb (all realized interactions across the entire spatial extent) is shown on the left. In the center is what a hypothetical ecologist samples at each site. Notice that although bears are observed co-occurring with both salmon and pike, there was never a direct observation of bears eating pike, even though they actually do. Therefore, this interaction between bears and pike is a false-negative.

distribution) is shown in fig. 2(A) for varying values of p_{fn} and illustrates a fundamental link between our ability to reliably say an interaction doesn't exist— p_{tn} —and the number of times N we have observed a given species. In addition, note that there is no non-zero p_{fn} for which we can ever *prove* that an interaction does not exist—no matter how many observations of non-interactions N we have, $p_{tn} < 1$.

From fig. 2(A) it is clear that the more often we see two species co-occurring, but *not interacting*, the more likely the interaction is a true-negative. This has several practical consequences: first it means negatives taken outside the overlap of the range of each species aren't informative because co-occurrence was not possible, and therefore neither was an interaction. Second, we can use this relation to compute the expected number of total observations needed to obtain a “goal” number of observations of a particular pair of species (fig. 2(B)). As an example, if we hypothesize that A and B do not interact, and we want to see species A and B both co-occurring and *not interacting* 10 times to be confident this is a true negative, then we need an expected 1000 observations of all species if the relative abundances of A and B are both 0.1.

Because the true FNR is latent, we can never actually be sure what the actual number of false-negatives in our data—however, we can use simulation to estimate the FNR for datasets of a given size using neutral models of observation. If some of the “worst-case” FNRs presented in fig. 2(A) seem unrealistically high, considering that species are observed in proportion to their relative abundance. In the next section we demonstrate that the distribution of abundance in ecosystems can lead to very high realized values of FNR (p_{fn}) simply as an artifact of sampling effort.

False-negatives as a product of relative abundance

We now show that the realized FNR changes drastically with sampling effort due to the intrinsic variation of the abundance of individuals of each species within a community. We do this by simulating the process of observation of species interactions, applied both to 243 empirical food webs from the Mangal database (Banville *et al.* 2021) and random food-webs generated using the niche model, a simple generative model of food-web structure that accounts for allometric scaling (Williams & Martinez 2000). Our neutral model of observation assumes each observed species is drawn in proportion to each species' abundance at that place and time. The abundance distribution of a community can be reasonably-well described by a log-normal distribution (Volkov *et al.* 2003). In addition to the log-normal distribution, we also tested the case where the abundance distribution is derived from power-law scaling $Z^{(\log(T_i)-1)}$ where T_i is the

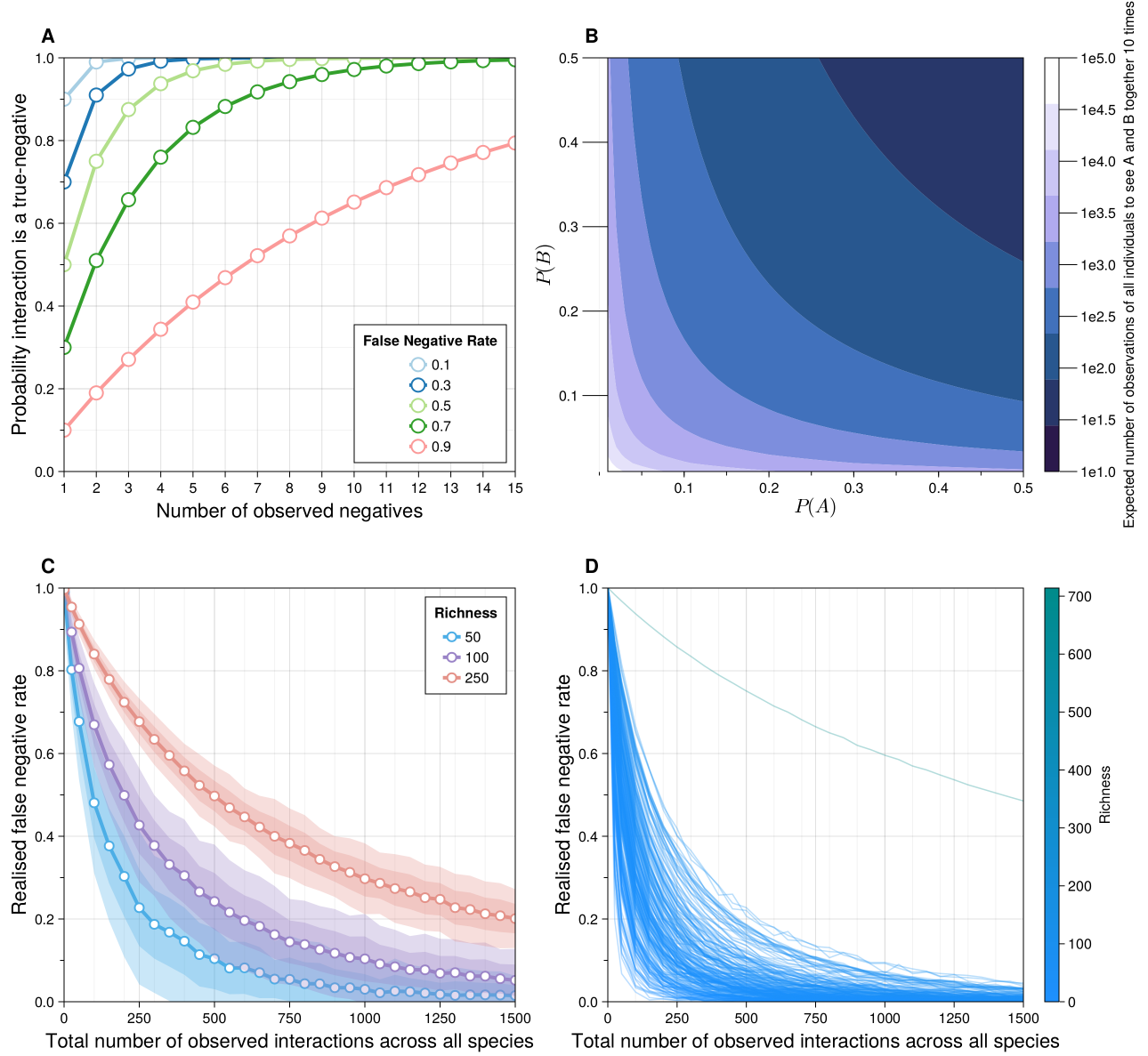


Figure 2: **(A)** The probability that an observed interaction is a true negative (y-axis) given how many times it has been sampled as a non-interaction (x-axis). Each color reflects a different value of p_{fn} , the false-negative-rate (FNR)—this is effectively the cumulative distribution function (cdf) of the geometric distribution. **(B)** The expected number of total observations needed (colors) to observe 10 co-occurrences between a species with relative abundance $P(A)$ (x-axis) and a second species with relative abundance $P(Y)$. **(C)**: false-negative-rate (y-axis) as a function of total sampling effort (x-axis) and network size, computed using the method described above. For 500 independent draws from the niche model (Williams & Martinez (2000)) at varying levels of species richness (colors) with connectance drawn according to the flexible-links model (MacDonald *et al.* (2020)) as described in the main text. For each draw from the niche model, 200 sets of 1500 observations are simulated, for which the mean false-negative-rate at each observation-step is computed. Means denoted with points, with 1 in the first shade and 2 in the second. **(D)**: Same as **(C)**, except using empirical food webs from Mangal database, where richness. The outlier on **(D)** is a 714 species food-web.

114 trophic level of species i and Z is a scaling coefficient (Savage *et al.* 2004), which yields the same
 115 qualitative behavior. The practical consequence of abundance distributions spanning many orders of
 116 magnitude of abundance is that observing two “rare” species interacting requires two low probability
 117 events: observing two rare species *at the same time*.

118 To simulate the process of observation, for an ecological network M with S species, we sample abundances
 119 for each species from a standard-log-normal distribution. For each true interaction in the adjacency matrix
 120 M (i.e. $M_{ij} = 1$) we estimate the probability of observing both species i and j at a given place and time by
 121 simulating n observations of all individuals of any a species, where the species of the individual observed
 122 at the $\{1, 2, \dots, n\}$ -th observation is drawn from the generated log-normal distribution of abundances. For
 123 each pair of species (i, j) , if both i and j are observed within the n -observations, the interaction is tallied as
 124 a true positive if $M_{ij} = 1$. If only one of i or j are observed—but not both—in these n observations, but
 125 $M_{ij} = 1$, this is counted as a false-negative, and a true-negative otherwise. For each pair of species (i, j) , if
 126 both i and j are observed within the n -observations, the interaction is tallied as a true positive if $M_{ij} = 1$.
 127 If only one of i or j are observed—but not both—in these n observations, but $M_{ij} = 1$, this is counted as a
 128 false-negative, and a true-negative otherwise ($M_{ij} = 0$). This process is illustrated conceptually in fig. 3(A).
 129 In fig. 2(C) we see this model of observation applied to niche model networks across varying levels of
 130 species richness, and in fig. 2(D) the observation model applied to Mangal food webs. For all niche model
 131 simulations in this manuscript, for a given number of species S the number of interactions is drawn from
 132 the flexible-links model fit to Mangal data (MacDonald *et al.* 2020), effectively drawing the number of
 133 interactions L for a random niche model food-web as

$$L \sim \text{BetaBinomial}(S^2 - S + 1, \mu\phi, 1 - \mu\phi)$$

134 where the maximum *a posteriori* (MAP) estimate of (μ, ϕ) applied to Mangal data from (MacDonald *et al.*
 135 2020) is $(\mu = 0.086, \phi = 24.3)$. All simulations were done with 500 independent replicates of unique niche
 136 model networks per unique number of observations n . All analyses presented here are done in Julia v1.8
 137 (Bezanson *et al.* 2015) using both EcologicalNetworks.jl v0.5 and Mangal.jl v0.4 (Banville *et al.* 2021) and
 138 are hosted on [Github](#)). Note that the empirical data, for the reasons described above, very likely already
 139 contains many false-negatives, we’ll revisit this issue in the final section.

140 From fig. 2(C) it is evident that the number of species considered in a study is inseparable from the

false-negative-rate in that study, and this effect should be taken into account when designing samples of ecological networks in the future. We see a similar qualitative pattern in fig. 2(D) where the FNR drops off quickly as a function of observation effort, mediated by total richness. The practical consequence of the bottom row of fig. 2 is whether the total number of observations of all species (the x-axis) for the threshold FNR we deem acceptable (the y-axis) is feasible. This raises two points: first, empirical data on interactions are subject to the practical limitations of funding and human-work hours, and therefore existing data tend to fall on the order of hundreds or thousands observations of individuals per site. Clear aggregation of data on sampling effort has proven difficult to find and a meta-analysis of network data and sampling effort seems both pertinent and necessary, in addition to the effects of aggregation of interactions across taxonomic scales (Gauzens *et al.* 2013; Giacomuzzo & Jordán 2021). This inherent limitation on in-situ sampling means we should optimize where we sample across space so that for a given number of samples, we obtain the maximum information possible. Second, what is meant by “acceptable” FNR? This raises the question: does a shifting FNR lead to rapid transitions in our ability inference and predictions about the structure and dynamics of networks, or does it produce a roughly linear decay in model efficacy? We explore this in the next section.

We conclude this section by advocating for the use of neutral models similar to above to generate expectations about the number of false-negatives in a data set of a given size. This could prove fruitful both for designing surveys of interactions but also because we may want to incorporate models of imperfect detection error into predictive interactions models, as Joseph (2020) does for species occurrence modeling. Additionally, we emphasize that one must consider the context for sampling—is the goal to detect a particular species (as in fig. 2(C)), or to get a representative sample of interactions across the species pool? These arguments are well-considered when sampling individual species (Willott 2001), but have not yet been adopted for designing samples of communities.

Including observation error in interaction predictions

Here we show how to incorporate uncertainty into model predictions of interaction probability to account for imperfect observation (both false-negatives and false-positives). Models for interaction prediction typically yield a probability of interaction between each pair of species, p_{ij} . When these are considered with uncertainty, it is usually model-uncertainty, e.g. the variance in the interaction probability prediction across several cross-validation folds, where the data is split into training and test sets several times. The

method we introduce adjusts the value of a model's predictions to produce a distribution of interaction probabilities, which are adjusted by a given false-negative-rate p_{fn} and false-positive-rate p_{fp} (outlined in figure fig. 3). We describe first how to sample from this distribution of adjusted interaction probabilities via simulation, and show that this distribution can be well-approximated analytically.

We then consider the output prediction from an arbitrary prediction model, which is the probability p_{ij} that two species i and j interact. To get an estimate of p_{ij} that accounts for observation error, we resample the probability of each interaction p_{ij} by simulating a set of several 'particles,' where each particle is a realization of an interaction occurring (either true or false with probabilities p_{ij} and $1 - p_{ij}$ respectively) and then being correctly observed with probabilities given by p_{fp} and p_{fn} to yield a single boolean outcome for each particle ("Resampling" within fig. 3 (B)). Across of many particles, the resulting frequency of 'true' outcomes is a single resample of the interaction probability p_{ij}^* . Across several samples each of several particles, this forms a distribution of probabilities which are adjusted by the true and false negative rates.

There is also an analytic way to approximate this distribution using the normal approximation to binomial. As a reminder, as the total number of samples N from a binomial distribution for n trials with success probability p from approaches infinity, the sum of total successes across all samples approaches a normal distribution with mean np and variance $np(1 - p)$. We can use this to correct the estimate p_{ij} based on the expected false-negative-rate p_{fn} and false-positive rate p_{fp} to obtain the limiting distribution as the number of resamples approaches infinity for the resampled p_{ij}^* for a given number of particles n_p . We do this by first adjusting for the rates of observation error to get the mean resampled probability, $\mathbb{E}[p_{ij}^*]$, as

$$\mathbb{E}[p_{ij}^*] = p_{ij}(1 - p_{fp}) + (1 - p_{ij})p_{fn}$$

which is obtainable by definition (supp 1.)

For notation, here we refer to a normal distribution with mean μ and standard-deviation σ as $\mathcal{N}(\mu, \sigma)$

Then yields the normal approximation

$$\sum_{i=1}^{n_p} p_{ij}^* \sim \mathcal{N}\left(n_p \cdot \mathbb{E}[p_{ij}^*], \sqrt{n_p \mathbb{E}[p_{ij}^*](1 - \mathbb{E}[p_{ij}^*])}\right)$$

which then can be converted back to a distribution of frequency of successes to yield the final

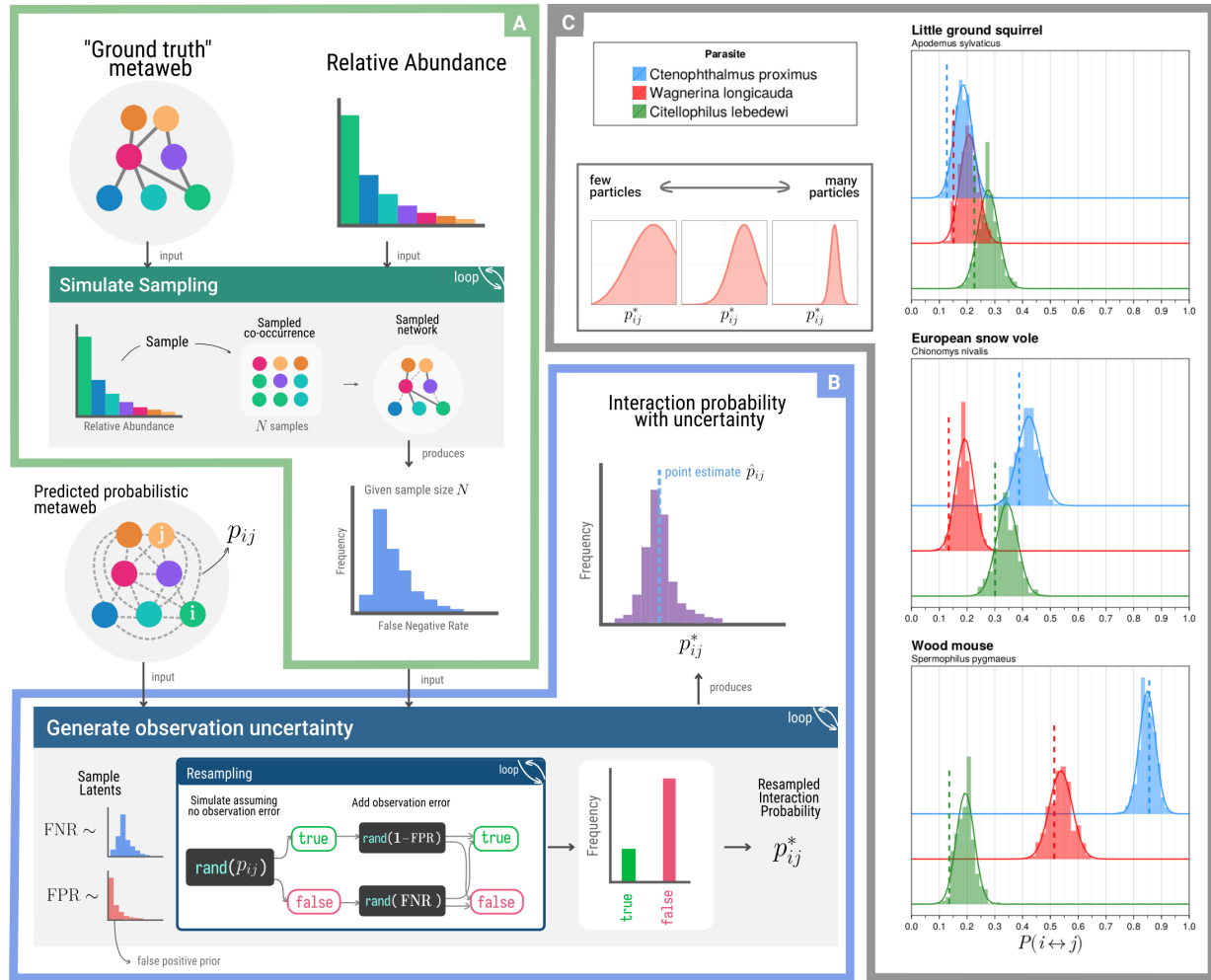


Figure 3: (A) The process for estimating the false-negative-rate (FNR) for an interaction dataset consisting of N total observed interactions. (B) The method for resampling interaction probability based on estimates of false-negative and false-positive rates. (C) The method for interaction probability resampling applied to three mammals and three parasites from the Hadfield *et al.* (2014) dataset. The original probability p_{ij} is indicated with a vertical dashed line. The histogram is simulated from the resampling process, and the line indicates the gaussian approximation to this distribution.

$$p_{ij}^* \sim \mathcal{N}\left(\mathbb{E}[p_{ij}^*], \sqrt{\frac{\mathbb{E}[p_{ij}^*](1 - \mathbb{E}[p_{ij}^*])}{n_p}}\right) \quad (1)$$

195 We can then further truncate this distribution to remain on the interval $(0, 1)$, as the output is a
 196 probability, although in practice often the probability mass outside $(0, 1)$ is extremely low except for p_{ij}
 197 values very close to 0 or 1. As an example case study, we use a boosted-regression-tree to predict
 198 interactions in a host-parasite network (Hadfield *et al.* 2014) (with features derived in the same manner as
 199 Strydom *et al.* (2021) derives features on this data) to produce a set of interaction predictions. We then
 200 applied this method to a set of a few resampled interaction probabilities between mammals and parasite
 201 species shown in figure fig. 3(C).

202 Why is this useful? For one, this analytic method avoids the extra computation required by simulating
 203 samples from this distribution directly. Further, it enables the extension of the natural analogue between
 204 n_p (the number of particles) and the number of observations of co-occurrence for a given pair of
 205 species—the fewer the particles, the higher the variance of the resulting approximation. The normal
 206 approximation is undefined for 0 particles (i.e. 0 observations co-occurrence), although as n_p approaches 0
 207 the approximated normal (once truncated) approaches the uniform distribution on the interval $(0, 1)$, the
 208 maximum entropy distribution where we have no information about the possibility of an interaction.

209 This also has implications for what we mean by ‘uncertainty’ in interaction predictions. A model’s
 210 prediction can be ‘uncertain’ in two different ways: (1) the model’s predictions may have high variance, or
 211 (2) the model’s predictions may be centered around a probability of interaction of 0.5, where we are the
 212 most unsure about whether this interaction exists. Improving the incorporation of different forms of
 213 uncertainty in probabilistic interaction predictions seems a necessary next step toward understanding
 214 what pairs of species we know the least about, in order to prioritize sampling to provide the most new
 215 information possible.

216 **Positive associations in co-occurrence increase the false-negative-rate**

217 The model above doesn’t consider the possibility that there are positive or negative associations which shift
 218 the probability of species cooccurrence away from what is expected based on their relative abundances due

219 to their interaction (Cazelles *et al.* 2016). However, here we demonstrate that the probability of having a
 220 false-negative can be higher if there is some positive association in the occurrence of species A and B . If
 221 we denote the probability that we observe the co-occurrence of two species A and B as $P(AB)$ and if there
 222 is no association between the marginal probabilities of observing A and observing B , denoted $P(A)$ and
 223 $P(B)$ respectively, then the probability of observing their co-occurrence is the product of the marginal
 224 probabilities for each species, $P(AB) = P(A)P(B)$. In the other case where there is some positive strength
 225 of association between observing both A and B because this interaction is “important” for each species,
 226 then the probability of observation both A and B , $P(AB)$, is greater than $P(A)P(B)$ as $P(A)$ and $P(B)$ are
 227 not independent and instead are positively correlated, i.e. $P(AB) > P(A)P(B)$. In this case, the probability
 228 of observing a single false-negative in our naive model from fig. 2(A) is $p_{fn} = 1 - P(AB)$, which due to the
 229 above inequality implies $p_{fn} > 1 - P(A)P(B)$. This indicates an increasingly greater probability of a false
 230 negative as the strength of association gets stronger, $P(AB) \rightarrow P(AB) \gg P(A)P(B)$. However, this still does
 231 not consider variation in species abundance in space and time (Poisot *et al.* 2015). If positive or negative
 232 associations between species structure variation in the distribution of $P(AB)$ across space/time, then the
 233 spatial/temporal biases induced by data collection would further impact the realized false-negative-rate, as
 234 the probability of false negative would not be constant for each pair of species across sites.

235 To test for these positive associations in data we scoured Mangal for datasets with many spatial or temporal
 236 replicates of the same system, which led to the resulting seven datasets set in figure fig. 4. For each
 237 dataset, we compute the marginal probability $P(A)$ of occurrence of each species A across all networks in
 238 the dataset. For each pair of interacting species A and B , we then compute and compare the probability of
 239 co-occurrence if each species occurs independently, $P(A)P(B)$, to the empirical joint probability of
 240 co-occurrence, $P(AB)$. Following our analysis above, if $P(AB)$ is greater than $P(A)P(B)$, then we expect
 241 our neutral estimates of the FNR above to underestimate the realized FNR. In fig. 4, we see the difference
 242 between $P(AB)$ and $P(A)P(B)$ for the seven suitable datasets with enough spatio-temporal replicates and a
 243 shared taxonomic backbone (meaning all individual networks use common species identifiers) found on
 244 Mangal to perform this analysis. Further details about each dataset are reported in tbl. 1.

245 In each of these datasets, the joint probability of co-occurrence $P(AB)$ is decisively greater than our
 246 expectation if species co-occur in proportion to their relative abundance $P(A)P(B)$. This suggests that
 247 there may not be as many “neutrally forbidden links” (Canard *et al.* 2012) as we might think, and that the
 248 reason we do not have records of interactions between rare species is probably due to observation error.

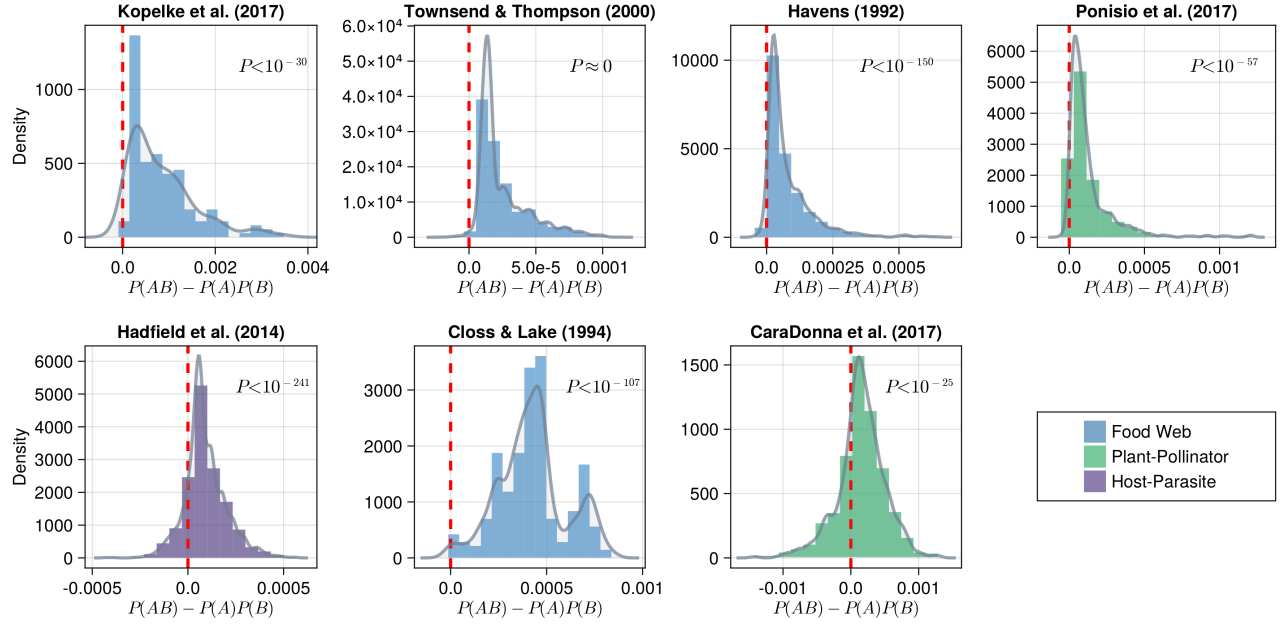


Figure 4: The difference between joint-probability of co-occurrence ($P(AB)$) and expected probability of co-occurrence under independence ($P(A)P(B)$) for interacting species for each dataset. The red-dashed line indicates 0 (no association). Each histogram represents a density, meaning the area of the entire curve sums to 1. The continuous density estimate (computed using local smoothing) is shown in grey. The p-value on each plot is the result of a one-sided t-test comparing the mean of each distribution to 0.

This has serious ramifications for the widely observed property of nestedness seen in bipartite networks (Bascompte & Jordano 2007)—perhaps the reason we have lots of observations between generalists is because they are more abundant, and this is particularly relevant as we have strong evidence that generalism drives abundance (Song *et al.* 2022a), not vice-versa.

Table 1: The datasets used in the above analysis (Fig 2). The table reports the type of each dataset, the total number of networks in each dataset (N), the total species richness in each dataset (S), the connectance of each metaweb (all interactions across the entire spatial-temporal extent) (C), the mean species richness across each local network \bar{S} , the mean connectance of each local network \bar{C} , the mean β -diversity among overlapping species across all pairs of network species ($\bar{\beta}_{OS}$), and the mean β -diversity among all species in the metaweb ($\bar{\beta}_{WN}$). Both metrics are computed using KGL β -diversity (Koleff *et al.* 2003)

Network	Type	N	S	C	\bar{S}	\bar{C}	$\bar{\beta}_{OS}$	$\bar{\beta}_{WN}$
Kopelke <i>et al.</i> (2017)	Food Web	100	98	0.037	7.87	0.142	1.383	1.972
Thompson & Townsend (2000)	Food Web	18	566	0.014	80.67	0.049	1.617	1.594
Havens (1992)	Food Web	50	188	0.065	33.58	0.099	1.468	1.881
Ponisio <i>et al.</i> (2017)	Pollinator	100	226	0.079	23.0	0.056	1.436	1.870
Hadfield <i>et al.</i> (2014)	Host-Parasite	51	327	0.085	32.71	0.337	1.477	1.952

Network	Type	N	S	C	\bar{S}	\bar{C}	$\bar{\beta}_{OS}$	$\bar{\beta}_{WN}$
Closs & Lake (1994)	Food Web	12	61	0.14	29.09	0.080	1.736	1.864
CaraDonna <i>et al.</i> (2017)	Pollinator	86	122	0.18	21.42	0.312	1.527	1.907

253 The impact of false-negatives on network properties and prediction

254 Here, we assess the effect of false-negatives on our ability to make predictions about interactions, as well
255 as their effect on network structure. The prevalence of false-negatives in data is the catalyst for interaction
256 prediction in the first place, and as a result methods have been proposed to counteract this bias (Stock *et*
257 *al.* 2017; Poisot *et al.* 2022). However, it is feasible that the FNR in a given dataset is so high that it could
258 induce too much noise for an interaction prediction model to detect the signal of possible interaction
259 between species.

260 To test this we use the dataset from Hadfield *et al.* (2014) that describes host-parasite interaction networks
261 sampled across 51 sites, and the same method as Strydom *et al.* (2021) to extract latent features for each
262 species in this dataset based on applying PCA to the co-occurrence matrix. We then predict a metaweb
263 (equivalent to predicting true or false for an interaction between each species pair, effectively a binary
264 classification problem) from these species-level features using four candidate models for binary
265 classification—three often used machine-learning (ML) methods (Boosted Regression Tree (BRT),
266 Random Forest (RF), Decision Tree (DT)), and one naive model from classic statistics (Logistic Regression
267 (LR)). Each of the ML models are bootstrap aggregated (or bagged) with 100 replicates each. We partition
268 the data into 80-20 training-test split, and then seed the training data with false negatives at varying rates,
269 but crucially do nothing to the test data. We fit all of these models using MLJ.jl, a high-level Julia
270 framework for a wide-variety of ML models (Blaom *et al.* 2020). We evaluate the efficacy of these models
271 using two common measures of binary classifier performance: the area under the receiver-operator curve
272 (ROC-AUC) and the area under the precision-recall curve (PR-AUC), for more details see Poisot (2022).
273 Here, PR-AUC is slightly more relevant as it is a better indicator of prediction of false-negatives. The
274 results of these simulations are shown in fig. 5(A&B).

275 One interesting result seen in fig. 5(A&B) is that the ROC-AUC value does not approach random in the
276 same way the PR-AUC curve does as we increase the added FNR. The reason for this is that ROC-AUC is



Figure 5: **(A)** The area-under the receiver-operator curve (ROC-AUC) and **(B)** The area-under the precision-recall curve (PR-AUC; right) for each different predictive model (colors/shapes) across a spectrum of the proportion of added false-negatives (x-axis). **(C)** The mean trophic-level of all species in a network generated with the niche model across different species richnesses (colors). For each value of the FNR, the mean trophic level was computed across 50 replicates. The shaded region for each line is one standard-deviation across those replicates.

277 fundamentally not as useful a metric in assessing predictive capacity as PR-AUC. As we keep adding more
278 false-negatives, the network eventually becomes a zeros matrix, and these models can still learn to predict
279 “no-interaction” for all possible species pairs, which does far better than random guessing (ROC-AUC =
280 0.5) in terms of the false positive rate (one of the components of ROC-AUC). This highlights a more broad
281 issue of label class imbalance, meaning there are far more non-interactions than interactions in data. A
282 full treatment of the importance of class-balance is outside the scope of this paper, but is explored in-depth
283 in Poisot (2022). Further we see, if anything, gradual decline in the performance of the model until we
284 reach very high FNR levels (i.e. $p_{fn} > 0.7$). This is consistent with other recent work (Gupta *et al.* 2023),
285 although it must be considered that the empirical data on which these models are trained already are
286 almost certain to already contain false-negatives.

287 Although these ML models are surprisingly performant at link prediction given their simplicity, there
288 have been several major developments in applying deep-learning methods to many tasks in network
289 inference and prediction—namely graph-representation learning (GRL, Khoshraftar & An (2022)) and
290 graph convolutional networks (Zhang *et al.* 2019). At this time, these advances can not yet be applied to
291 ecological networks because they require far more data than we currently have. We already have lots of
292 features that could be used as inputs into these models (i.e. species level data about occurrence, genomes,
293 abundance, etc.), but our network datasets barely get into the hundreds of local networks sampled across
294 space and time (tbl. 1). Once we start to get into the thousands, these models will become more useful, but
295 this can only be done with systematic monitoring of interactions. This again highlights the need to
296 optimize our sampling effort to maximize the amount of information contained in our data given the
297 expense of sampling interactions.

298 We also consider how the FNR affects network properties. In fig. 5(C) we see the mean trophic level across
299 networks simulated using the niche model (as above), across a spectrum of FNR values. In addition to the
300 clear dependence on richness, we see that mean trophic level, despite varying widely between niche model
301 simulations, tends to be relatively robust to false-negatives and does not deviate widely from the true value
302 until very large FNRs. This is not entirely unsurprising. Removing links randomly from a food-web is
303 effectively the inverse problem of the emergence of a giant component (more than half of the nodes are in
304 a connected network) in random graphs (see Li *et al.* (2021) for a thorough review). The primary
305 difference being that we are removing edges, not adding them, and thus we are witnessing the dissolution
306 of a giant component, rather than the emergence of one. Further applications of percolation theory (Li *et*

307 *al.* 2021) to the topology of sampled ecological networks could improve our understanding of how
308 false-negatives impact the inferences about the structure and dynamics on these networks.

309 Discussion

310 Species interactions enable the persistence and functioning of ecosystems, but our understanding of
311 interactions is limited due to the intrinsic difficulty of sampling them. Here we have provided a null
312 model for the expected number of false-negatives in an interaction dataset. We demonstrated that we
313 expect many false-negatives in species interaction datasets purely due to the intrinsic variation of
314 abundances within a community. We also, for the first time to our knowledge, measured the strength of
315 association between co-occurrence and interactions (Cazelles *et al.* 2016) across many empirical systems,
316 and found that these positive associations are both very common, and showed algebraically that they
317 increase the realized FNR. We have also shown that false-negatives could further impact our ability to
318 both predict interactions and infer properties of the networks, which highlights the need for further
319 research into methods for correcting this bias in existing data.

320 A better understanding of how false-negatives impact species interaction data is a practical
321 necessity—both for inference of network structure and dynamics, but also for prediction of interactions by
322 using species level information. False-negatives could pose a problem for many forms of inference in
323 network ecology. For example, inferring the dynamic stability of a network could be prone to error if the
324 observed network is not sampled “enough.” What exactly “enough” means is then specific to the
325 application, and should be assessed via methods like those here when designing samples. Further,
326 predictions about network rewiring (Thompson & Gonzalez 2017) due to range shifts in response to
327 climate change could be error-prone without accounting for interactions that have not been observed but
328 that still may become climatically infeasible. As is evident from fig. 2(A), we can never guarantee there are
329 no false-negatives in data. In recent years, there has been interest toward explicitly accounting for
330 false-negatives in models (Stock *et al.* 2017; Young *et al.* 2021), and a predictive approach to
331 networks—rather than expecting our samples to fully capture all interactions (Strydom *et al.* 2021). As a
332 result, better models for predicting interactions are needed for interaction networks. This includes
333 explicitly accounting for observation error (Johnson & Larremore 2021)—certain classes of models have
334 been used to reflect hidden states which account for detection error in occupancy modeling (Joseph 2020),

and could be integrated in the predictive models of interactions in the future.

This work has several practical consequences for the design of surveys for species' interactions. Simulating the process of observation could be a powerful tool for estimating the sampling effort required by a study that takes relative abundance into account, and provides a null baseline for expected FNR. It is necessary to take the size of the species pool into account when deciding how many total samples is sufficient for an "acceptable" FNR (fig. 2(C & D)). Further the spatial and temporal turnover of interactions means any approach to sampling prioritization must be spatiotemporal. We demonstrated earlier that observed negatives outside of the range of both species aren't informative, and therefore using species distribution models could aid in this spatial prioritization of sampling sites.

We also should address the impact of false-negatives on the inference of process and causality in community ecology. We demonstrated that in model food webs, false-negatives do not impact the measure of total trophic levels until very high FNR (figure fig. 5(C)), although we cannot generalize this further to other properties. This has immediate practical concern for how we design what taxa to sample—does it matter if the sampled network is fully connected? It has been shown that the stability of subnetworks can be used to infer the stability of the metaweb paper beyond a threshold of samples (Song *et al.* 2022b). But does this extend to other network properties? And how can we be sure we are at the threshold at which we can be confident our sample characterizes the whole system? We suggest that modeling observation error as we have done here can address these questions and aid in the design of samples of species interactions. To try to survey to avoid all false-negatives is a fool's errand. Species ranges overlap to form mosaics, which themselves are often changing in time. Communities and networks don't end in space, and the interactions that connect species on the 'periphery' of a given network to species outside the spatial extent of a given sample will inevitably appear as false-negatives in practical samples. The goal should instead be to sample a system enough to have a statistically robust estimate of the current state and empirical change over time of an ecological community at a given spatial extent and temporal resolution, and to determine what the sampling effort required should be prior to sampling.

Our work highlights the need for a quantitatively robust approach to sampling design, both for interactions (Jordano 2016) and all other aspects of biodiversity (Carlson *et al.* 2020). As anthropogenic forces create rapid shifts in our planet's climate and biosphere, this is an imperative to maximize the amount of ecological information we get in our finite samples, and make our inferences and decisions based on this data as robust as possible. Where we choose to sample, and how often we choose to sample

365 there, has strong impacts on the inferences we make from data. Incorporating a better understanding of
366 sampling effort and bias to the design of biodiversity monitoring systems, and the inference and predictive
367 models we apply to this data, is imperative in understanding how biodiversity is changing, and making
368 forecasts that can guide conservation action.

369 **Acknowledgements**

370 AG & MDC acknowledge the support of the Liber Ero Chair for Biodiversity conservation and NSERC.

371 **References**

- 372 Banville, F., Vissault, S. & Poisot, T. (2021). Mangal.jl and EcologicalNetworks.jl: Two complementary
373 packages for analyzing ecological networks in Julia. *Journal of Open Source Software*, 6, 2721.
- 374 Bascompte, J. & Jordano, P. (2007). Plant-Animal Mutualistic Networks: The Architecture of Biodiversity.
375 *Annual Review of Ecology, Evolution, and Systematics*, 38, 567–593.
- 376 Becker, D.J., Albery, G.F., Sjodin, A.R., Poisot, T., Bergner, L.M., Dallas, T.A., *et al.* (2021). Optimizing
377 predictive models to prioritize viral discovery in zoonotic reservoirs.
- 378 Bezanson, J., Edelman, A., Karpinski, S. & Shah, V.B. (2015). Julia: A Fresh Approach to Numerical
379 Computing.
- 380 Blanchet, F.G., Cazelles, K. & Gravel, D. (2020). Co-occurrence is not evidence of ecological interactions.
381 *Ecology Letters*, 23, 1050–1063.
- 382 Blaom, A.D., Kiraly, F., Lienart, T., Simillides, Y., Arenas, D. & Vollmer, S.J. (2020). MLJ: A Julia package
383 for composable machine learning. *Journal of Open Source Software*, 5, 2704.
- 384 Boakes, E.H., Rout, T.M. & Collen, B. (2015). Inferring species extinction: The use of sighting records.
385 *Methods in Ecology and Evolution*, 6, 678–687.
- 386 Canard, E., Mouquet, N., Marescot, L., Gaston, K.J., Gravel, D. & Mouillot, D. (2012). Emergence of
387 Structural Patterns in Neutral Trophic Networks. *PLOS ONE*, 7, e38295.

388 CaraDonna, P.J., Petry, W.K., Brennan, R.M., Cunningham, J.L., Bronstein, J.L., Waser, N.M., *et al.* (2017).
389 Interaction rewiring and the rapid turnover of plantpollinator networks. *Ecology Letters*, 20, 385–394.

390 Carlson, C.J., Dallas, T.A., Alexander, L.W., Phelan, A.L. & Phillips, A.J. (2020). What would it take to
391 describe the global diversity of parasites? *Proceedings of the Royal Society B: Biological Sciences*, 287,
392 20201841.

393 Cazelles, K., Araújo, M.B., Mouquet, N. & Gravel, D. (2016). A theory for species co-occurrence in
394 interaction networks. *Theoretical Ecology*, 9, 39–48.

395 Closs, G.P. & Lake, P.S. (1994). Spatial and Temporal Variation in the Structure of an Intermittent-Stream
396 Food Web. *Ecological Monographs*, 64, 1–21.

397 de Aguiar, M.A.M., Newman, E.A., Pires, M.M., Yeakel, J.D., Boettiger, C., Burkle, L.A., *et al.* (2019).
398 Revealing biases in the sampling of ecological interaction networks. *PeerJ*, 7, e7566.

399 Gauzens, B., Legendre, S., Lazzaro, X. & Lacroix, G. (2013). Food-web aggregation, methodological and
400 functional issues. *Oikos*, 122, 1606–1615.

401 Giacomuzzo, E. & Jordán, F. (2021). Food web aggregation: Effects on key positions. *Oikos*, 130,
402 2170–2181.

403 Griffiths, D. (1998). Sampling effort, regression method, and the shape and slope of sizeabundance
404 relations. *Journal of Animal Ecology*, 67, 795–804.

405 Gupta, A., Figueroa H., D., O’Gorman, E., Jones, I., Woodward, G. & Petchey, O.L. (2023). How many
406 predator guts are required to predict trophic interactions? *Food Webs*, 34, e00269.

407 Hadfield, J.D., Krasnov, B.R., Poulin, R. & Nakagawa, S. (2014). A Tale of Two Phylogenies: Comparative
408 Analyses of Ecological Interactions. *The American Naturalist*, 183, 174–187.

409 Havens, K. (1992). Scale and Structure in Natural Food Webs. *Science*, 257, 1107–1109.

410 Johnson, E.K. & Larremore, D.B. (2021). Bayesian estimation of population size and overlap from random
411 subsamples.

412 Jordano, P. (2016). Sampling networks of ecological interactions. *Functional Ecology*, 30, 1883–1893.

413 Joseph, M.B. (2020). Neural hierarchical models of ecological populations. *Ecology Letters*, 23, 734–747.

414 Kenall, A., Harold, S. & Foote, C. (2014). An open future for ecological and evolutionary data? *BMC*
415 *Evolutionary Biology*, 14, 66.

416 Khoshraftar, S. & An, A. (2022). A Survey on Graph Representation Learning Methods.

417 Koleff, P., Gaston, K.J. & Lennon, J.J. (2003). Measuring beta diversity for presence-absence data. *Journal*
418 *of Animal Ecology*, 72, 367–382.

419 Kopelke, J.-P., Nyman, T., Cazelles, K., Gravel, D., Vissault, S. & Roslin, T. (2017). Food-web structure of
420 willow-galling sawflies and their natural enemies across Europe. *Ecology*, 98, 1730–1730.

421 Li, M., Liu, R.-R., Lü, L., Hu, M.-B., Xu, S. & Zhang, Y.-C. (2021). Percolation on complex networks:
422 Theory and application. *Physics Reports*, Percolation on complex networks: Theory and application,
423 907, 1–68.

424 MacDonald, A.A.M., Banville, F. & Poisot, T. (2020). Revisiting the Links-Species Scaling Relationship in
425 Food Webs. *Patterns*, 1.

426 Makiola, A., Compson, Z.G., Baird, D.J., Barnes, M.A., Boerlijst, S.P., Bouchez, A., *et al.* (2020). Key
427 Questions for Next-Generation Biomonitoring. *Frontiers in Environmental Science*, 7.

428 Martinez, N.D., Hawkins, B.A., Dawah, H.A. & Feifarek, B.P. (1999). Effects of Sampling Effort on
429 Characterization of Food-Web Structure. *Ecology*, 80, 1044–1055.

430 McLeod, A., Leroux, S.J., Gravel, D., Chu, C., Cirtwill, A.R., Fortin, M.-J., *et al.* (2021). Sampling and
431 asymptotic network properties of spatial multi-trophic networks. *Oikos*, 130, 2250–2259.

432 Moore, A.L. & McCarthy, M.A. (2016). Optimizing ecological survey effort over space and time. *Methods*
433 *in Ecology and Evolution*, 7, 891–899.

434 Niedballa, J., Wilting, A., Sollmann, R., Hofer, H. & Courtiol, A. (2019). Assessing analytical methods for
435 detecting spatiotemporal interactions between species from camera trapping data. *Remote Sensing in*
436 *Ecology and Conservation*, 5, 272–285.

437 Paine, R.T. (1988). Road Maps of Interactions or Grist for Theoretical Development? *Ecology*, 69,
438 1648–1654.

439 Poisot, T. (2022). Guidelines for the prediction of species interactions through binary classification.

440 Poisot, T., Bergeron, G., Cazelles, K., Dallas, T., Gravel, D., MacDonald, A., *et al.* (2021). Global knowledge
 441 gaps in species interaction networks data. *Journal of Biogeography*, 48, 1552–1563.

442 Poisot, T., Ouellet, M.-A., Mollentze, N., Farrell, M.J., Becker, D.J., Brierly, L., *et al.* (2022). Network
 443 embedding unveils the hidden interactions in the mammalian virome.

444 Poisot, T., Stouffer, D.B. & Gravel, D. (2015). Beyond species: Why ecological interaction networks vary
 445 through space and time. *Oikos*, 124, 243–251.

446 Ponisio, L.C., Gaiarsa, M.P. & Kremen, C. (2017). Opportunistic attachment assembles plantpollinator
 447 networks. *Ecology Letters*, 20, 1261–1272.

448 Savage, V.M., Gillooly, J.F., Brown, J.H., West, G.B. & Charnov, E.L. (2004). Effects of Body Size and
 449 Temperature on Population Growth. *The American Naturalist*, 163, 429–441.

450 Song, C., Simmons, B.I., Fortin, M.-J. & Gonzalez, A. (2022a). Generalism drives abundance: A
 451 computational causal discovery approach. *PLOS Computational Biology*, 18, e1010302.

452 Song, C., Simmons, B.I., Fortin, M.-J., Gonzalez, A., Kaiser-Bunbury, C.N. & Saavedra, S. (2022b). Rapid
 453 monitoring for ecological persistence.

454 Stephenson, P. (2020). Technological advances in biodiversity monitoring: Applicability, opportunities
 455 and challenges. *Current Opinion in Environmental Sustainability*, Open issue 2020 part A: Technology
 456 Innovations and Environmental Sustainability in the Anthropocene, 45, 36–41.

457 Stock, M., Poisot, T., Waegeman, W. & De Baets, B. (2017). Linear filtering reveals false negatives in
 458 species interaction data. *Scientific Reports*, 7, 45908.

459 Strydom, T., Catchen, M.D., Banville, F., Caron, D., Dansereau, G., Desjardins-Proulx, P., *et al.* (2021). A
 460 roadmap towards predicting species interaction networks (across space and time). *Philosophical
 461 Transactions of the Royal Society B: Biological Sciences*, 376, 20210063.

462 Thompson, P.L. & Gonzalez, A. (2017). Dispersal governs the reorganization of ecological networks under
 463 environmental change. *Nature Ecology & Evolution*, 1, 1–8.

464 Thompson, R.M. & Townsend, C.R. (2000). Is resolution the solution?: The effect of taxonomic resolution
 465 on the calculated properties of three stream food webs. *Freshwater Biology*, 44, 413–422.

466 Volkov, I., Banavar, J.R., Hubbell, S.P. & Maritan, A. (2003). Neutral theory and relative species abundance
 467 in ecology. *Nature*, 424, 1035–1037.

- 468 Walther, B.A., Cotgreave, P., Price, R.D., Gregory, R.D. & Clayton, D.H. (1995). Sampling Effort and
469 Parasite Species Richness. *Parasitology Today*, 11, 306–310.
- 470 Williams, R.J. & Martinez, N.D. (2000). Simple rules yield complex food webs. *Nature*, 404, 180–183.
- 471 Willott, S.j. (2001). Species accumulation curves and the measure of sampling effort. *Journal of Applied*
472 *Ecology*, 38, 484–486.
- 473 Young, J.-G., Valdovinos, F.S. & Newman, M.E.J. (2021). Reconstruction of plantpollinator networks from
474 observational data. *Nature Communications*, 12, 3911.
- 475 Zhang, S., Tong, H., Xu, J. & Maciejewski, R. (2019). Graph convolutional networks: A comprehensive
476 review. *Computational Social Networks*, 6, 11.